Lateral Organization and Domain Formation in a Two-Component Lipid Membrane System

Chad Leidy,* Willem F. Wolkers,* Kent Jørgensen,†‡ Ole G. Mouritsen,‡ and John H. Crowe*

*Biophysics and Structural Biology Graduate Group, Section of Molecular and Cellular Biology, University of California, Davis, Davis, California 95616 USA; †Department of Pharmaceutics, The Royal Danish School of Pharmacy, DK-2100, Copenhagen, Denmark; and ‡Department of Chemistry, Technical University of Denmark, DK-2800, Lyngby, Denmark

ABSTRACT The thermodynamic phase behavior and lateral lipid membrane organization of unilamellar vesicles made from mixtures of 1,2-dimyristoyl-*sn*-glycero-3-phosphocholine (DMPC) and 1,2 distearoyl-*sn*-glycero-3-phosphocholine (DSPC) were investigated by fluorescence resonance energy transfer (FRET) as a function of temperature and composition. This was done by incorporating a headgroup-labeled lipid donor (NBD-DPPE) and acceptor (N-Rh-DPPE) in low concentrations into the binary mixtures. Two instances of increased energy transfer efficiency were observed close to the phase lines in the DMPC/DSPC phase diagram. The increase in energy transfer efficiency was attributed to a differential preference of the probes for dynamic and fluctuating gel/fluid coexisting phases. This differential preference causes the probes to segregate (S. Pedersen, K. Jørgensen, T. R. Baekmark, and O. G. Mouritsen, 1996, *Biophys. J.* 71:554–560). The observed increases in energy transfer match with the boundaries of the DMPC/DSPC phase diagram, as measured by Fourier transform infrared spectroscopy (FTIR) and differential scanning calorimetry (DSC). We propose that the two instances of probe segregation are due to the presence of DMPC-rich and DSPC-rich domains, which form a dynamic structure of gel/fluid coexisting phases at two different temperatures. Monitoring the melting profile of each lipid component independently by FTIR shows that the domain structure is formed by DMPC-rich and DSPC-rich domains rather than by pure DMPC and DSPC domains.

INTRODUCTION

Lipid domains in biological and model membranes have been studied intensively in recent years (e.g., Welti and Glaser, 1994; Mouritsen and Jørgensen, 1997; Brown and London, 1998; Stillwell et al., 2000) and have recently been observed in giant unilamellar vesicles (Korlach et al., 1999; Bagatolli and Gratton, 2000a,b). Domain formation has been shown to be relevant in biological functions (Bergelson et al., 1995), including, for example, enzymatic activity of phospholipase A_2 (PLA_2), which has been related to dynamic coexisting gel/fluid domains and lipid bilayer microheterogeneity (Hønger et al., 1996); activity of protein kinase C (PKC) and diglucosyldiacylglycerol (DiGlcDAG) synthase, which were shown to increase due to the formation of domains rich in diacylglycerides acting as enzymatic activators (Dibble et al., 1996; Karlsson et al., 1996); and vesicle budding and membrane trafficking, which have been suggested to be influenced by dynamic domain formation (Verkade and Simons, 1997; Mukherjee et al., 1999). The importance of lipid domains in several biological processes emphasizes the need to understand the factors that regulate their formation, stability, and in particular, the relevant size and time scales of the small-scale lipid structures formed.

Membrane domains display a broad range of size scales, from the micrometer to the nanometer range. Domains in the micrometer range include whole patches of the cell membrane and can be directly visualized by light microscopy (Hwang et al., 1998). Domain formation at the mesoscale (nanometer range) is more difficult to study because domain sizes are beyond the resolution of standard light microscopy techniques, and their formation is more dynamic in nature (Mouritsen and Jørgensen, 1994). Nevertheless, there is indirect evidence of their existence (Sankaram et al., 1992; Schram et al., 1996; Jørgensen et al., 1996), and several experiments have corroborated their biological relevance (Melo et al., 1992; Bergelson et al., 1995; Clerc and Thompson, 1995; Hønger et al., 1996).

Simple lipid binary systems have been intensively used as models to understand the formation of nanoscale domains. Visualizing the formation of heterogeneous gel/fluid domain structures has been achieved in supported monolayers and bilayers (Möhwald et al., 1995; Hollars and Dunn, 1998), where large lipid domains can be directly observed by fluorescence microscopy. Recently, direct visualization of lipid domains in the nanometer range has been reported by atomic force microscopy in simple lipid bilayers and monolayers (Gliss et al., 1998; Nielsen et al., 2000). Due to the resolution constraints in detecting nanoscale domains, several spectroscopic and fluorescent techniques have been used to provide indirect evidence of the existence and behavior of nanoscale lipid domains in nonsupported lipid bilayers. For example, fluorescence recovery after photobleaching (FRAP) has been used in binary systems composed of lipids with different acyl chain lengths to study the connectivity of the fluid phase at different temperatures and compositions (Vaz et al., 1990; Schram et al., 1996). Additional information has been obtained with the use of electron paramagnetic resonance (EPR) (Sankaram et al.,

Received for publication 27 March 2000 and in final form 4 January 2001.

Address reprint requests to Dr. Chad Leidy, Section of Molecular and Cellular Biology, University of California, Davis, CA 95616. Tel.: 530-752-1094; Fax: 530-752-5305; E-mail: ccleidy@ucdavis.edu.

0006-3495/01/04/1819/10 $2.00

1992), which was used to determine that, for a 1,2-dimyristoyl-sn-glycero-3-phosphocholine (DMPC)/1,2-distearoyl-sn-glycero-3-phosphocholine (DSPC) system, the number of lipid molecules per gel domain increased linearly from a fixed number of nucleation sites with increasing gel phase fraction. Fourier transform infrared (FTIR) spectroscopy has been used to study phase separation, and the formation of small domains, with the use of acyl-chain deuterated lipids (Mendelsohn and Moore, 1998). Formation of small domains on the order of 50 molecules can be monitored through the splitting of the CH_2 scissoring mode (Mendelsohn et al., 1995). Fluorescence quenching has been used to provide evidence for the formation of a liquid ordered phase at physiological temperatures in model systems (Ahmed et al., 1997; Silvius et al., 1996). Eximer to monomer fluorescence emission ratio was utilized to study domain formation due to hydrophobic mismatch (Lehtonen et al., 1996), and the non-ideal mixing in PC-ceramide binary mixtures (Holopainen et al., 1997).

In the current work we have expanded on a fluorescence energy transfer (FRET) technique used previously to study a one-component lipid system (Pedersen et al., 1996). In this previous study, the dynamic formation of nanoscale domains in DPPC bilayers was monitored by following the energy transfer between a donor and an acceptor fluorescent probe pair (NBD and rhodamine headgroup-labeled lipids) incorporated into the bilayer. Recent evidence showed that these probes partition almost equally between the gel and liquid-crystalline phases (Mesquita et al., 2000). In particular, the partitioning coefficient between gel and liquid-crystalline phases for the NBD-labeled probe we used in this study was measured to be 1.0–1.1. Nevertheless, the probes do show slight differences in their preference for either of these phases (Pedersen et al., 1996), which can be advantageous in studying membrane phase separation. We propose that the differential affinity induces the probes to segregate into coexisting gel and fluid domains when the two phases are present in the coexistence temperature range. The proximity and interaction between the probes can be monitored by the quenching of the donor probe due to energy transfer to the acceptor. In the temperature range where only one phase is present in the bilayer system, the probes remain well mixed, leading to quenching. In the range of the transition temperature, gel and fluid domains coexist dynamically, and the probes segregate due to their differential affinity for the gel and fluid coexisting phases, thereby reducing the energy transfer from the donor to the acceptor manifested as an increase in the fluorescence of the donor. Due to the strong distance-dependent (r^{-6}) decay in the efficiency of energy transfer (Stryer, 1978), this technique is sensitive to domain formation on the order of 10 nm. Previous results using this technique in DPPC bilayers show a maximum in the fluorescence at the DPPC phase transition temperature, which indicates the presence of a heterogeneous gel/fluid lipid domain structure (Pedersen et al., 1996).

We used a donor acceptor system of NBD-DPPE/N-Rh-DPPE probes to monitor domain formation in a DMPC/DSPC binary mixture. By following the segregation of the probes as it is manifested by the temperature-dependent changes in energy transfer, we provide additional insight into the microstructure properties of the DMPC/DSCP binary mixture. As shown previously by differential scanning calorimetry (DSC), the DMPC/DSPC mixture is characterized by a broad gel-fluid phase coexistence region limited by two phase boundaries (Mabrey and Sturtevant, 1976). The non-ideal mixing properties of this system make the DMPC/DSPC binary mixture a good model for understanding phase separation and lipid domain formation. FTIR spectroscopy and DSC were used to complement the fluorescence data. A good correlation was found between the three techniques in determining the DMPC/DSPC phase diagram.

MATERIALS AND METHODS

The phospholipids DMPC, DSPC, deuterated 1,2-dimyristoyl-d54-*sn*-glycero-3-phosphocholine (DMPC-d54), and the fluorescent probes 1,2-dipalmitoyl-*sn*-glycero-d-phosphoethanolamine-N-(7-nitro-2–1,3-benzoxadiazol-4-yl) (NBD-DPPE), 1,2-dimyristoyl-d54-*sn*-glycero-3-phosphoethanolamine-N-(7-nitro-2–1,3-benzoxadiazol-4-yl) (NBD-DMPE), 1,2-dipalmitoyl-*sn*-glycero-3-phosphoethanolamine-N-(lissamine rhodamine B sulfonyl) (N-Rh-DPPE), 1,2-dimyristoyl-*sn*-glycero-3-phosphoethanolamine-N-(lissamine rhodamine B sulfonyl) (N-Rh-DMPE), and 1-palmitoyl-2-[6-[(7-nitro-2–1,-3-benzoxadiazol-4-yl)amino]caproyl]-*sn*-glycero-3-phosphocholine (NBD C6-HPC) were purchased from Avanti Polar Lipids (Alabaster, AL) and were used without further purification. Appropriate amounts of DSPC, DMPC, and the fluorescent probes were dissolved and mixed in chloroform. The concentration of each probe in the membrane was 0.25 mol %. The samples were then dried under nitrogen gas and placed under vacuum overnight to remove the residual solvent. The dry lipids were dispersed in 0.1 mM EGTA and 10 mM TES buffer (pH 7.2) to a final concentration of 50 mM (~30 mg/ml). Aqueous multilamellar lipid dispersions were prepared by heating the sample to 65°C, followed by vortexing. This procedure was repeated multiple times for a total of 20 min. Large unilamellar vesicles were prepared by extruding the suspension 15 times through a hand-held Lipofast extruder (Avestin, Ottawa, Canada) with two stacked 0.1-μm pore size polycarbonate filters (Poretics, Livermore, CA). Multilamellar lipid dispersions at a concentration of 50 mg/ml were used for the FTIR measurements.

FRET measurements

Fluorescence measurements were performed on a Hitachi F-2000 fluorescence spectrophotometer. The excitation and emission wavelengths used were 470 nm and 530 nm, corresponding to the excitation and emission wavelengths for the NBD-DPPE donor. For the fluorescence measurements, 0.5 ml of a 1:10 dilution aliquot (5 mM) of the original sample was placed in a temperature-controlled cuvette holder regulated by an external water bath. Measurements were obtained at a scan rate of 30°C/h. The temperature of the sample was directly measured by insertion of a thermocouple into the cuvette.

Differential scanning calorimetry measurements

DSC was performed with a high-sensitivity DSC from Calorimetry Science Corp. (Provo, UT) with nitrogen gas purge. The scanning rates for all measurements were 30°C/h. The sample size was 0.2 ml of a 5 mM lipid suspension. A baseline correction was performed by subtracting a measurement of the pans without the lipid suspension. The onset and completion temperatures used to compose the DMPC/DSPC phase diagram were determined by intersecting the slope line at half-width of the peak heat capacity and the baseline (Mabrey and Sturtevant, 1976).

FTIR measurements and analysis

IR spectra were recorded on a Perkin-Elmer 2000 Fourier transform IR-spectrometer (Perkin-Elmer, Norwalk, CT) equipped with a liquid-nitrogen-cooled mercury/cadmium/telluride (MCT) detector interfaced to a microcomputer with Spectrum 2000 software. A 5-μl volume of sample at 50 mg/ml lipid concentration was placed between two FTIR CaF_2 windows. Temperature was controlled by a Peltier device and monitored by a thermocouple placed on the FTIR window. Infrared spectra in the CH_2 stretching region from 3000 to 2800 cm^{-1}, and CD_2 stretching region from 2200 to 2000 cm^{-1} were monitored as a function of temperature. Eight spectra were averaged at each temperature point. Spectra were continuously acquired at a temperature increase rate of 3°C/min. Phase transitions were determined by plotting the band positions of the CH_2 symmetric and CD_2 asymmetric stretch modes. The band positions were determined by taking the inverted second derivative of the original spectra and averaging the band intercepts at 80% intensity. The symmetric CD_2 stretch mode is less intense than the asymmetric mode, and it appears as a poorly defined shoulder for the lipid concentrations studied. Therefore, to obtain a less noisy phase transition measurement we followed the more intense asymmetric CD_2 stretching vibration for the deuterated species. Conversely, we used the symmetric CH_2 stretch mode to monitor phase transitions for nondeuterated species, because this mode is more widely used for nondeuterated lipids. There appears to be no appreciable difference between measurements of the phase transition using the symmetric and asymmetric CH_2 stretch modes.

RESULTS

Fig. 1 *A* shows fluorescence intensity as a function of temperature for a NBD-DPPE probe incorporated into 50/50 DMPC/DSPC unilamellar vesicles in the presence and absence of N-Rh-DPPE (all DMPC/DSPC ratios given are molar ratios). A decay in the emission fluorescence as a function of temperature is observed in the sample containing only NBD-DPPE. This has been previously reported for NBD-PE incorporated into CHO cells (Chapman et al., 1995) and DPPC liposomes (Pedersen et al., 1996), and a decrease in NBD quantum yield with temperature has been measured for several NBD derivatives in a variety of organic solvents (Fery-Forgues et al., 1993). A similar decay in the N-Rh-PE emission fluorescence with increasing temperature is observed for vesicles incorporated with N-Rh-PE acceptor only (data not shown). In general, a decrease in fluorescence emission with increasing temperature has been reported for several fluorescent probes (Oliver et al., 2000).

When both probes are present, the fluorescence emission of NBD-DPPE is quenched by N-Rh-DPPE, as is evident in Fig. 1 *A* by the overall reduced fluorescence level (lower trace). A variety of mechanisms of interaction could be responsible for the observed quenching, although energy transfer is assumed to be the most likely mechanism. The degree of quenching of the NBD-DPPE probe by N-Rh-DPPE varies throughout the temperature range in a nonmonotonous manner. Two well-defined maxima in the fluorescence intensity are observed during both heating and cooling scans at 31°C and 44°C. The absence of any maxima in the sample containing only NBD-DPPE indicates that these maxima are the result of an increased segregation and a decreased average interaction between the donor and acceptor probes.

Fig. 1 *B* shows the trace that results from ratioing the NBD plus N-Rh-PE fluorescence (lower trace) by the NBD only fluorescence (upper trace), which is done to account for the temperature dependence of the NBD-DPPE fluores-

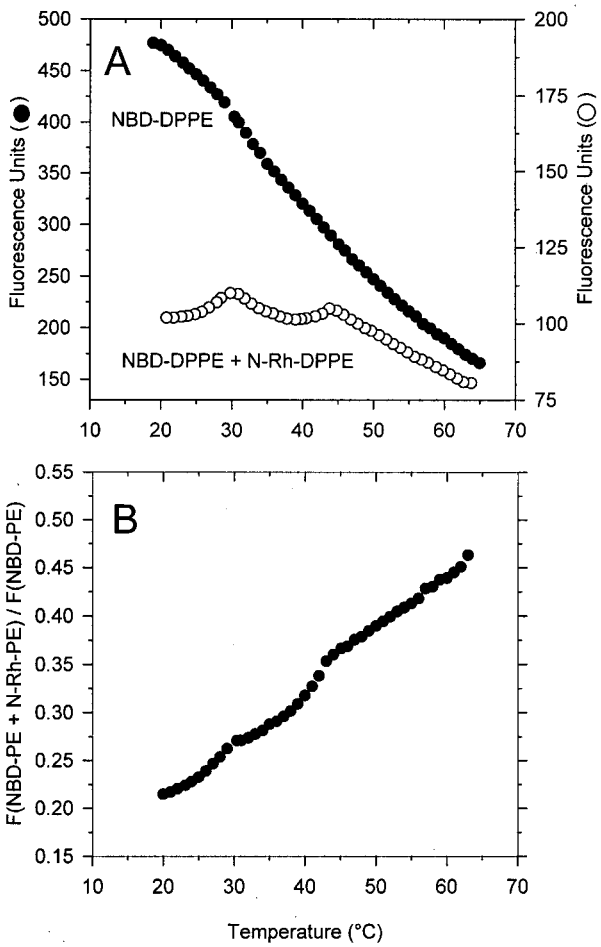

FIGURE 1 (*A*) Temperature dependence of NBD-DPPE emission fluorescence intensity obtained for unilamellar 50:50 DMPC:DSPC vesicles incorporated with 0.25 mol % of NBD-DPPE only (*upper trace*) and 0.25 mol % of NBD-DPPE and N-Rh-DPPE (*lower trace*). (*B*) Trace obtained by ratioing the NBD-DPPE fluorescence emission in the presence of N-Rh-DPPE (*lower trace*, *A*) versus the absence of N-Rh-DPPE (*upper trace*, *A*). The excitation and emission wavelengths were 470 nm and 530 nm. Results were obtained at a scan rate of 30°C/h.

cence. The two features observed in the lower trace in Fig. 1 *A*, although less prevalent, are still present after correcting for the NBD thermal dependence. However, the overall positive slope observed makes it difficult to assess if the features still represent true maxima in the energy transfer in a sloping baseline, or if there is a continuous segregation of the probes with increasing temperature. Fig. 1 *B* shows a positive slope even above 50°C where the system is completely in the fluid phase. This implies that the positive slope is caused not only by a continual segregation of the probes with increasing temperature but also by changes in the energy transfer efficiency with increasing temperature. The excited-state lifetime of NBD-PE incorporated into DLPC and DSPC vesicles has been shown to decrease with increasing temperature (Loura et al., 2000). This effect would decrease the energy transfer efficiency between the two probes and is one of the factors that could account for the positive slope observed.

Overall, Fig. 1 suggests that the NBD-DPPE and N-Rh-DPPE probes undergo a higher degree of segregation at two discrete temperatures close to the phase lines in the DMPC/DSPC mixture, implying that the average interaction between the probes is sensitive to the temperature-dependent domain structure of the DMPC/DSPC binary mixture.

In Fig. 2 the positions of the maxima in the fluorescence quenching (*a*) are compared with the phase transition temperatures as measured by DSC (*b*) and FTIR (*c* and *d*) for a 60/40 DMPC/DSPC sample. The melting profile for the DMPC/DSPC binary system shows two cooperative transitions, evident from the two peaks in the heat flow as measured by DSC (Fig. 2 *b*). This indicates non-ideal mixing for this lipid system. Partial mixing of the two lipids causes the cooperative transitions to shift closer together (31°C and 44°C) compared with the observed positions in the pure state (25°C and 55°C). The peaks in the heat capacity as measured by DSC closely match the peaks in fluorescence as measured by FRET (Fig. 2 *a*).

With FTIR, the phase transition can be monitored as a sharp shift in the wavenumber of the acyl chain stretching vibration as the lipids undergo a transition from an ordered to a disordered conformation. The acyl chain stretching vibrations for each lipid can be resolved with the use of acyl chain deuterated DMPC-d54 and nondeuterated DSPC. This allows us to follow the conformational state of the DMPC and DSPC lipids independently (Mendelsohn and Moore, 1998). The asymmetric CD_2 stretching vibration indicates the conformational state of the DMPC molecules, and the symmetric CH_2 stretching vibration indicates the conformational state of the DSPC molecules. The wavenumber versus temperature plot of the CD_2 stretching vibration shows that the DMPC lipids start melting a few degrees lower than what is observed by FRET and DSC (Fig. 2). This is partly due to the lower phase transition temperature of the deuterated DMPC compared with non-deuterated DMPC. A previous study showed that DPPC-d62 has a phase transition

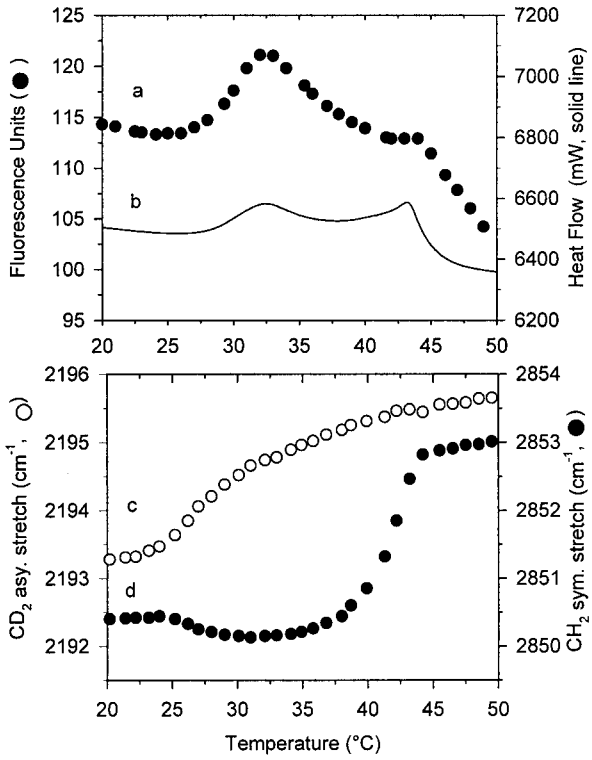

FIGURE 2 Comparison of thermotropic phase transition measurements between FRET (*a*), DSC (*b*), DMPC-d54 CD_2 asymmetric stretch (ranging from 2193 cm^{-1} to 2196 cm^{-1}) (*c*), and DSPC CH_2 symmetric stretch (ranging from 2850 cm^{-1} to 2854 cm^{-1}) (*d*) for a 60/40 DMPC:DSPC molar ratio.

temperature that is 6°C lower than non-deuterated DPPC (Mendelsohn and Koch, 1980). We expect a similar shift for deuterated DMPC.

Fig. 2 shows that the fluorescence quenching results match closely with the phase transitions as measured by both DSC and FTIR. This result suggests that maximum segregation of the probes occurs close to the lower solidus and upper liquidus phase boundaries, indicating that at these two temperatures there is a fluctuating and dynamic coexistence of gel and liquid-crystalline phases.

Fig. 3 *A* shows fluorescence quenching for various compositions of the DMPC/DSPC lipid mixtures. The position and relative intensities of the fluorescence maxima vary with composition ratio. The pure DMPC and DSPC samples show single peaks in the fluorescence at 25°C and 55°C, respectively, corresponding to the main phase transition temperature for the individual lipid components. With increasing DSPC mole fractions, the two peaks in the fluorescence shift toward higher temperatures. In addition, there is a decrease in the magnitude of the lower temperature fluorescence peak and a concomitant increase in the higher temperature peak with increasing DSPC fraction. The maxima in fluorescence intensity (Fig. 3 *A*) correlate very well with the cooperative transitions as measured by DSC (Fig. 3 *B*) and FTIR (Fig. 3, *C* and *D*).

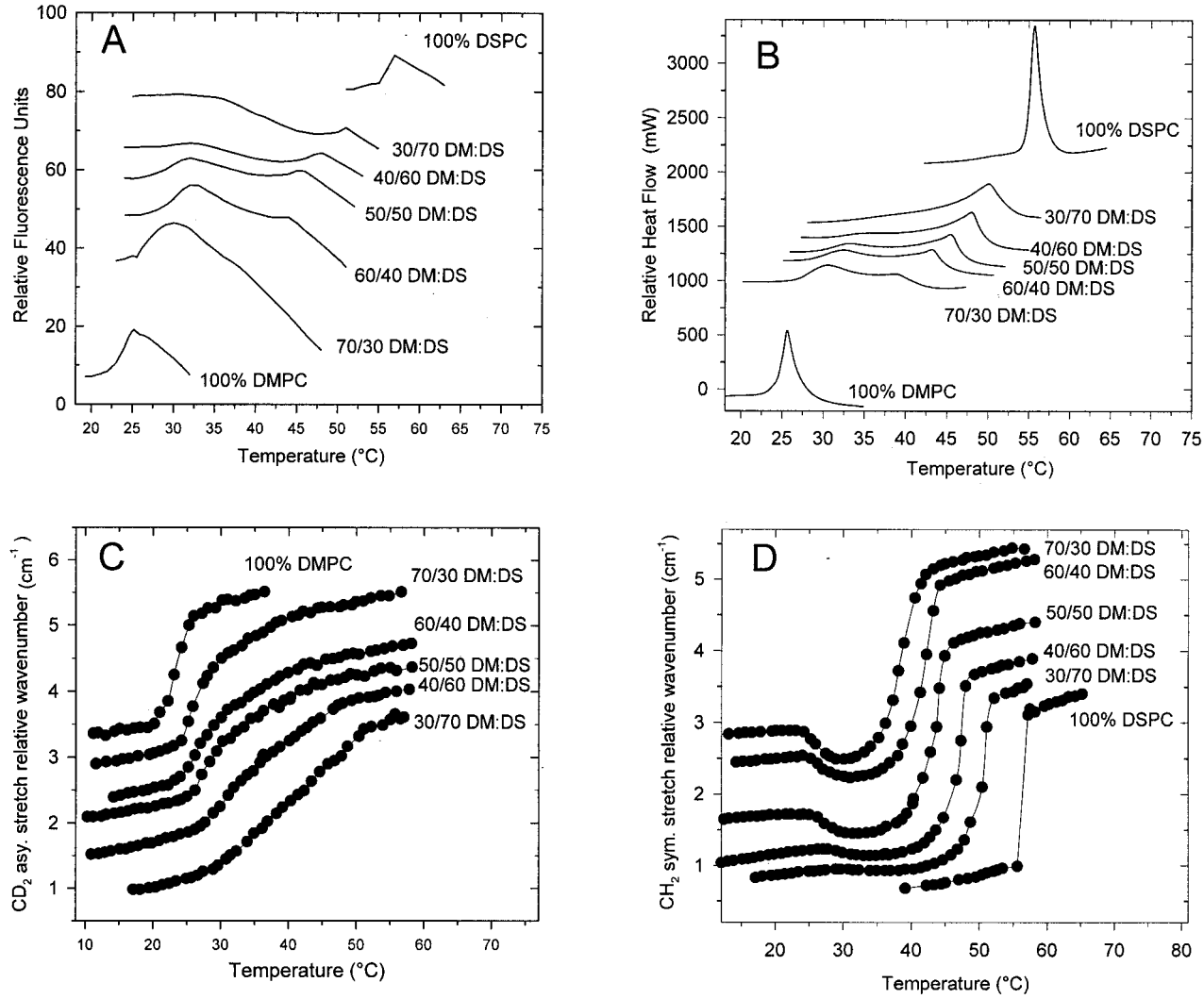

FIGURE 3 FRET (*A*), DSC (*B*), DMPC-d54 CD_2 asymmetric stretch (*C*), and DSPC CH_2 symmetric stretch (*D*) measurements as a function of temperature obtained for increasing DMPC/DSPC ratios. Mole ratios are shown on graphs. FTIR results were plotted as relative wavenumber.

In Figs. 4 and 5 we performed a more detailed examination of the FTIR results through first-derivative analysis of the wavenumber versus temperature plots. In Fig. 4, a 70:30 DMPC-d54/DSPC sample shows clearly that DMPC-d54 (Fig. 4 *A*) and DSPC (Fig. 4 *B*) reach their midpoint of transition at 26°C and 41°C, respectively. Interestingly, at 26°C, where a major part of the DMPC-d54 molecules melt (Fig. 4 *A*), the DSPC CH_2 stretch mode shows a sharp decrease in wavenumber (Fig. 4 *B*). We suggest that this drop in wavenumber indicates that the DSPC molecules become more closely packed as the DMPC-d54 molecules undergo melting.

In Fig. 5, a 40:60 DMPC-d54/DSPC sample shows cooperative transitions at 31°C and 43°C for DMPC-d54 (Fig. 5 *A*) and DSPC (Fig. 5 *B*), respectively. DMPC-d54 shows a second, smaller cooperative transition at 43°C, suggesting that a small population of DMPC-d54 molecules melts at the same temperature as the bulk DSPC population. This result also supports the hypothesis that a small population of DMPC-d54 molecules is incorporated into DSPC-rich regions.

In Fig. 6 we present a phase diagram for the DMPC/DSPC binary mixture constructed from the DSC data for different lipid ratios. The solidus and liquidus phase boundaries are estimated by taking the onset and completion temperatures from the DSC thermograms for increasing DMPC/DSPC ratios (solid line). The fluorescence intensity maxima closely trace the cooperative phase changes as measured by DSC for the different DMPC/DSPC ratios. The solidus phase boundary as measured by FTIR appears to be a few degrees lower than what is observed with the other two techniques. This is again due to the lower phase transition temperature of the deuterated DMPC used in the FTIR measurements. Overall, the results show that maxi-

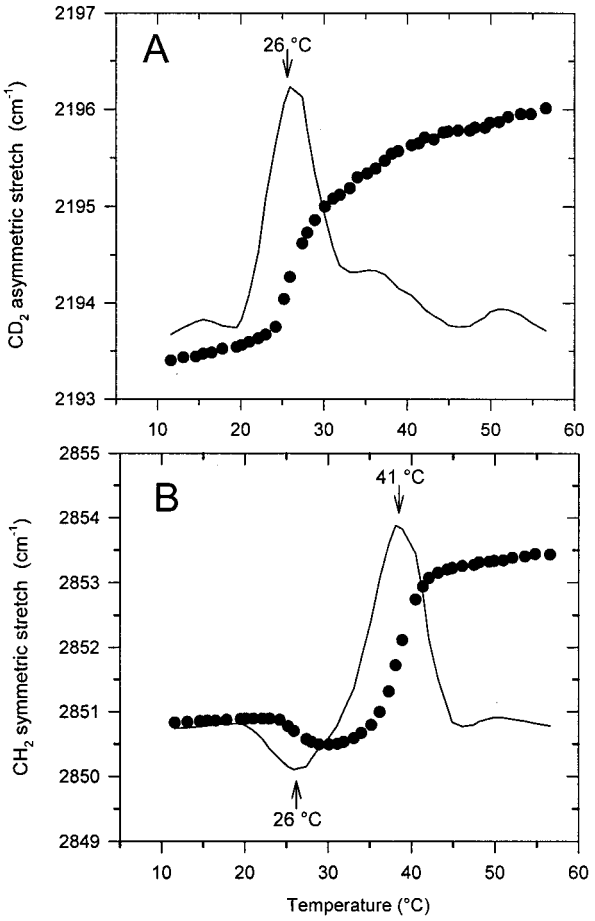

FIGURE 4 Wavenumber versus temperature plots (●) and first derivative of wavenumber versus temperature plots (——) of the DMPC-d54 CD_2 asymmetric stretch (*A*) and the DSPC CH_2 symmetric stretch (*B*) of a 70:30 DMPC-d54:DSPC mixture.

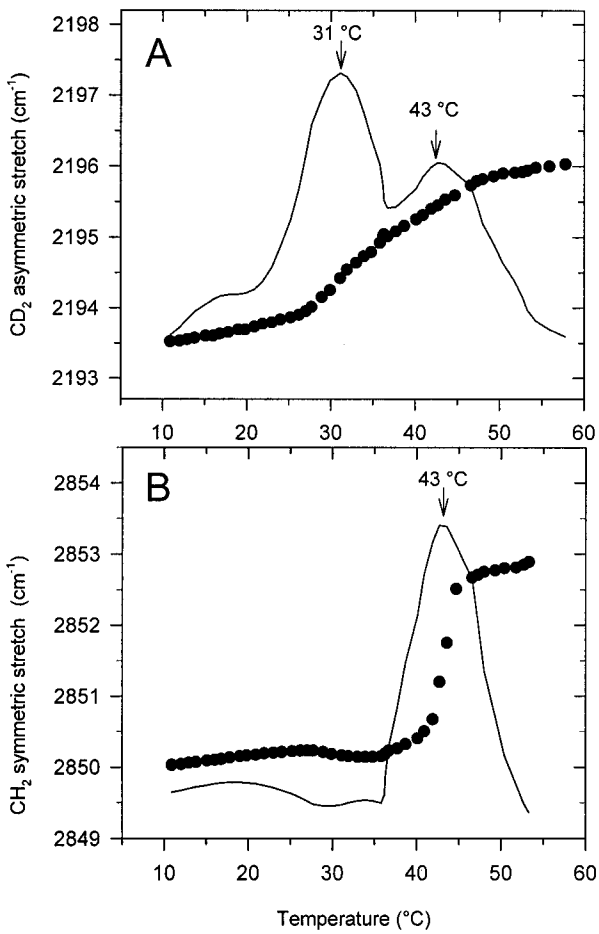

FIGURE 5 Wavenumber versus temperature plots (●) and first derivative of wavenumber versus temperature plots (——) of the DMPC-d54 CD_2 asymmetric stretch (*A*) and the DSPC CH_2 symmetric stretch (*B*) of a 40:60 DMPC-d54:DSPC mixture.

mum probe segregation occurs during the two instances of cooperative phase changes in the DMPC/DSPC system.

In Fig. 7 different combinations of probes were incorporated into a 50/50 DMPC/DSPC sample to explore in more depth the factors that affect probe segregation. In Fig. 7 *A*, 50/50 DMPC/DSPC samples were incorporated with three different probe combinations with varying acyl chain lengths, NBD-DPPE and N-Rh-DPPE (top trace), NBD-DMPE and N-Rh-DMPE (middle trace), and NBD-DMPE and N-Rh-DPPE (bottom trace). For the middle trace, the probes were chosen to have the same chain length as DMPC. The fluorescence for the middle trace displays a less pronounced maximum at the solidus phase boundary compared with the top trace. On the other hand, at the liquidus phase boundary for the middle trace a similar maximum in fluorescence appears. This implies that for the probes that resemble the DMPC chain length, their ability to segregate is diminished at the solidus phase boundary where mainly DMPC lipids become disordered.

For the lower trace in Fig. 7 *A*, the probes are chosen with different chain lengths, using NBD-DMPE and N-Rh-DPPE. The solidus phase boundary shows a similar maximum in fluorescence as seen in the top trace. The liquidus phase boundary shows a less pronounced maximum as compared with the top trace, indicating that this probe combination has a reduced ability to segregate at the liquidus phase boundary temperature where the DSPC lipids become disordered.

In Fig. 7 *B* we explore the effect of probe mobility on segregation. The probes used in Fig. 1 have high mobility in the fluid phase. However, the mobility of the probes is known to drop sharply in the gel phase (Schram et al., 1996). To assess how the low mobility of the probes in the gel phase influences probe segregation, we incorporated a probe, NBD C_6-HPC, that shows relatively higher mobility in the gel phase in combination with N-Rh-DPPE into a 50/50 DMPC/DSPC sample. The NBD C_6-HPC is a chain-labeled probe that moves rapidly between the water and the

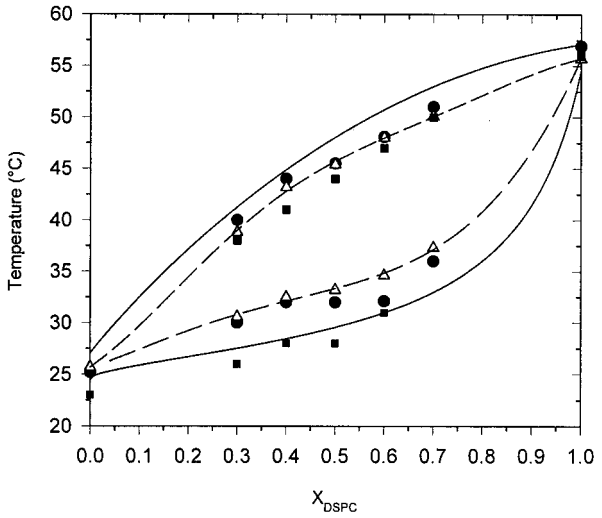

FIGURE 6 Measurements of T_{m1} and T_{m2} in a DMPC/DSPC temperature-composition diagram as detected by FRET (●), DSC (△), and FTIR (■). The phase boundaries (——) for the DMPC/DSPC phase diagram were defined by the onset and completion temperatures determined by DSC. Melting curves (— — —) are defined by the position of T_{m1} and T_{m2} measured by DSC.

lipid phase (Nichols and Pagano, 1981). This, in addition to its relatively short chain length, allows the probe to have higher mobility than the headgroup-labeled probes and should allow for less restrictive movement between fluid and gel phases and domains. The upper trace in Fig. 7 *B* shows a broad maximum in the fluorescence ranging throughout the gel/fluid coexistence region as determined by DSC. Superimposed on this broad maximum are the two less pronounced peaks. This shows that with the more mobile probe, segregation is minimal in the gel phase, increasing as the overall gel/fluid ratio approaches 50/50, then decreasing again as the fluid phase is reached.

DISCUSSION

The FRET results obtained for the DMPC/DSPC mixture (Fig. 1) show probe segregation at two distinct temperatures, reflecting the DMPC/DSPC phase boundaries. The fluorescence results correlate very well with the DMPC and DSPC cooperative transitions as measured by DSC and FTIR.

In a previous study with the same donor-acceptor pair incorporated into a pure DPPC system, a maximum in the donor fluorescence was observed at the DPPC main phase transition (Pedersen et al., 1996). Those workers proposed that the maximum in fluorescence is caused by segregation of the probes due to their differential partitioning between coexisting fluid and gel domains, which form at the DPPC phase transition, and which are dynamic and fluctuating in character. We base our interpretation on this model; however, other scenarios that could explain the increase in fluorescence at the phase boundaries should also be considered. For example, a similar temperature-dependent segregation could arise if the probes were first clustered at low temperatures due to exclusion from the gel phase and were then diluted into an increasing fluid phase with increasing temperature. The two distinct increases in fluorescence at the phase boundaries could be related to a sharper increase in fluid phase at those temperatures. However, recent experiments with headgroup-labeled phospholipids with the same chain lengths as the probes used here show that NBD-PE partitions close to equally between the gel and fluid phases (Mesquita et al., 2000). Although the Mesquita et al. results imply that clustering of the probes due to exclusion from the gel phase is unlikely, the results do not exclude the possibility that the probes might cluster as they partition into the gel phase. The observed segregation can also be explained by one of the fluorophores having a stronger preference than the other fluorophore for localizing at the gel/liquid-crystalline interphase. An increase in the overall gel/liquid-crystalline interface would induce a decrease in energy transfer. A recent report measuring FRET between NBD-PE and 1,1′-didodecil-3-3-3′,3′-tetramethylindocarbocyanine (DiI) incorporated in a two-lipid bilayer system suggests that DiI partitions into the gel/liquid-crystalline interface (Loura et al., 2000). If this were the case maximum segregation between the probes would be observed when the interface is maximized. Recent Monte Carlo simulations on a DMPC/DSPC system suggest that the gel/liquid-crystalline interface reaches a plateau close to the phase boundaries (Sugar et al., 1999). Although it is difficult to distinguish between segregation induced by differential partitioning between the gel and liquid-crystalline phases and preference of one of the fluorophores for the interface, both of these scenarios indicate the presence of coexisting liquid-crystalline/gel domains. We suggest, then, that a maximum in the donor fluorescence is indication of dynamic and fluctuating gel/liquid-crystalline domain coexistence at the nanoscale level, as suggested by Monte Carlo simulations (Pedersen et al., 1996).

If we consider that the DMPC/DSPC phase diagram is characterized by a broad fluid/gel coexistence region, and that energy transfer is sensitive only to the proportion of liquid-crystalline and gel phases, only a single peak in the fluorescence intensity would be expected to occur at one temperature between both liquidus and solidus phase lines. This is where the gel and fluid phases are present in equal proportion and where the system is expected to display macroscopic gel/liquid-crystalline phase segregation. The presence of two peaks (Fig. 1 *A*) in the donor fluorescence is surprising. Our results suggest that segregation of the probes occurs at two distinct temperatures close to the phase lines in the DMPC/DSPC system and not at an intermediate temperature in the coexistence temperature range. A possible interpretation we propose is the sequential melting of a larger domain structure composed of DMPC-rich and

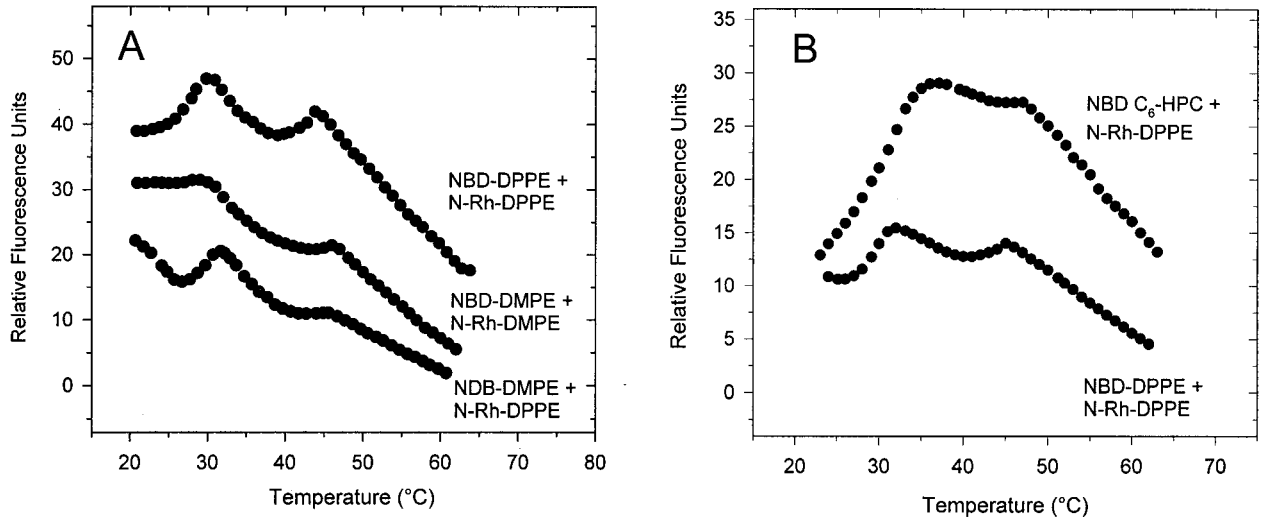

FIGURE 7 (*A*) Differences in temperature dependence of NBD-PE fluorescence emission for several NBD-PE/N-Rh-PE donor/acceptor pairs with varying chain lengths incorporated into 50/50 DMPC:DSPC large unilamellar vesicles. Chain lengths are indicated in the graph. (*B*) Temperature dependence of NBD-PE fluorescence emission obtained for a highly mobile probe NBD-C_6-HPC incorporated with N-Rh-DPPE in unilamellar 50/50 DMPC/DSPC vesicles (*upper trace*), compared with NBD-DPPE incorporated with N-Rh-DPPE in 50/50 DMPC/DSPC vesicles (*lower trace*). All probe concentrations in the vesicles are 0.25 mol %.

DSPC-rich lipid domains. This is apparent from the fact that the lower temperature fluorescence maximum corresponds to the DMPC phase transition, and the higher temperature fluorescence maximum corresponds to the DSPC phase transition, as measured by FTIR (Fig. 2). We propose that, in the heating direction, the DMPC-rich domains would form a structure of coexisting gel and fluid domains first, resulting in a maximum in the fluorescence close to the solidus phase boundary when the fluorescent probes located in these domains segregate. The fluorescent probes in the DSPC domains would be confined to the DSPC-rich gel phase and would not be mobile enough during the characteristic fluorescence lifetime to move into the DMPC domains during the lower cooperative transition. The probes contained in the DSPC gel phase would remain immobile until the higher-temperature phase line is reached and a dynamic fluctuating coexistence of gel and fluid phases is formed as the DSPC-rich domains melt, allowing for a second instance of probe segregation.

We chose a chain-labeled NBD probe (NBD-C_6-HPC) with high mobility in the gel phase and high affinity for the fluid phase to evaluate the effect of probe mobility on the fluorescence results. The result in Fig. 7 *B* clearly shows that probe mobility leads to a broader temperature profile of the fluorescence than observed in Fig. 1 *A*, suggesting that the more mobile NBD probe partitions into the growing fluid phase and is not restrained in the DSPC-rich gel phase. In this case, probe segregation is more closely related to the relative percentages of gel and fluid phases in the bilayer, in which case probe segregation is expected to reach a maximum at a temperature where the gel and fluid phases reach equal proportions. Two less pronounced maxima at each of the phase transition temperatures were still observed, although the broad fluorescence profile is prevalent.

The FTIR results show that the DMPC and DSPC molecules undergo independent cooperative transitions matching the fluorescence maxima (Fig. 2), suggesting the presence of DMPC and DSPC domains. As expected from the partial mixing behavior of this system (Mabrey and Sturtevant, 1976), the FTIR results also show that these domains are not formed purely of DMPC or DSPC but are doped with a smaller population of the other lipid. This is clear from Fig. 5, which shows a small population of DMPC molecules melting during the DSPC cooperative transition. The drop in wavenumber of the DSPC molecules during the DMPC cooperative transition (Fig. 4) suggests that the DSPC molecules become more ordered as the DMPC molecules melt. A possible interpretation for this drop in wavenumber is that, as the DMPC domains melt, the small population of DSPC molecules located in the DMPC regions migrate to the DSPC regions. As a result, the DSPC molecules become more ordered, and their average wavenumber drops. Both results (Figs. 4 and 5) suggest the coexistence of DMPC-rich and DSPC-rich domains.

It is important to stress that the two maxima in the fluorescence are obtained in both heating and cooling directions. It has been suggested for several lipid systems that a heterogeneous structure is present in the fluid phase (Knoll et al., 1981; Ruggiero and Hudson, 1989; Nielsen et al., 1999). This would imply that a DMPC-rich phase and a DSPC-rich phase, with their respective populations of fluorophores, would remain present throughout the tempera-

ture range. Alternatively, if the system becomes well mixed in the fluid phase, a more dynamic interpretation is necessary to explain the two instances of probe segregation that occur in the cooling direction. This interpretation would have to account for the de-mixing of the DMPC and DSPC molecules into a domain structure as the system is cooled. A recent Monte Carlo simulation of the DMPC/DSPC mixture measures the probability of finding fluid/gel lipid pairs as a function of temperature, which is interpreted as the phase boundary of the system (Sugar et al., 1999). The measurements show that the total number of fluid/gel lipid pairs (DMPC/DSPC plus DMPC/DMPC plus DSPC/DSPC) reaches a threshold value at the phase transition temperatures and remains level for intermediate temperatures. Moreover, the simulation also shows that the number of fluid/gel pairs for each species (DMPC/DMPC and DSPC/DSPC) reaches a maximum at their respective phase transition temperatures. This suggests that the probe segregation maxima observed in Fig. 1 are related to the presence of DMPC fluid-gel pairs near the solidus and DSPC fluid/gel pairs near the liquidus phase lines. We believe that the dynamic and fluctuating nature of the coexisting gel-fluid phases close to the phase boundaries is what allows for the efficient segregation of the probes. However, it is not clear whether the binary lipid model system used in this simulation study (Sugar et al., 1999) displays a macroscopic fluid-gel phase coexistence. From this evidence we propose that in the cooling direction, DSPC-rich gel domains are nucleated first in the cooling scans, producing a maximum in the phase boundary, and a maximum in probe segregation close to the liquidus phase line. This would be followed by nucleation of DMPC-rich gel domains with maximum segregation obtained at a temperature close to the solidus phase boundary. The end result would be a heterogeneous domain structure formed by DMPC-rich and DSPC-rich domains in the gel phase (Jørgensen et al., 1993).

The fluorescence setup used in the present study demonstrates the usefulness of the donor-acceptor system for studying lipid membrane microstructure. The same technique has recently been used to study domain formation in docosahexaenoic-acid-rich bilayers (Stillwell et al., 2000) and in other binary systems (Loura et al., 2000). The level of probe segregation appears to be sensitive to the presence of heterogeneous lipid domain structures near the phase boundaries in this lipid mixture. The sensitivity to bilayer heterogeneity in this FRET setup can be useful in detecting domain formation in other lipid systems. In particular, this could be achieved by an appropriate choice of fluorescent probes with specific preferences to the domain systems of interest. In addition, the technique was used to accurately predict the DMPC/DSPC phase diagram and was found to be in excellent agreement with DSC and FTIR results. This shows that FRET is a useful tool in mapping out phase diagrams for a variety of lipid systems, which might be helpful in cases where other techniques cannot be used, such as in the case of critical mixing points in lipid-cholesterol mixtures.

Supported by grants NHLBI 57810–01 from National Institutes of Health and N66001–00-C-8048 from Defense Advanced Research Projects Agency, by a National Science Foundation Graduate Fellowship, by the Danish Center for Drug Design and Transport, and by the Hasselblad Foundation.

REFERENCES

Ahmed, S. N., D. A. Brown, and E. London. 1997. On the origin of sphingolipid/cholesterol-rich detergent-insoluble cell membranes: physiological concentrations of cholesterol and sphingolipid induce formation of a detergent-insoluble, liquid-ordered lipid phase in model membranes. *Biochemistry.* 36:10944–10953.

Bagatolli, L. A., and E. Gratton. 2000a. Two-photon fluorescence microscopy of coexisting lipid domains in giant unilamellar vesicles of binary phospholipid mixtures. *Biophys. J.* 78:290–305.

Bagatolli, L. A., and E. Gratton. 2000b. A correlation between lipid domain shape and binary phospholipid mixture composition in free standing bilayers: a two-photon fluorescence microscopy study. *Biophys. J.* 79: 434–447.

Bergelson, L. O., K. Gawrisch, J. A. Ferretti, and R. Blumenthal. 1995. Special Issue on Domain Organization in Biological Membranes. *Mol. Membr. Biol.* 12:1–162.

Brown, D. A., and E. London. 1998. Structure and origin of ordered lipid domains in biological membranes. *J. Membr. Biol.* 164:103–114.

Chapman, C. F., Y. Liu, G. J. Sonek, and B. J. Tromberg. 1995. The use of exogenous fluorescent measurements in single living cells. *Photochem. Photobiol.* 62:416–425.

Clerc, S. G., and T. E. Thompson. 1995. Permeability of dimyristoyl phosphatidylcholine/dipalmitoyl phosphatidylcholine bilayer membranes with coexisting gel and liquid-crystalline phases. *Biophys. J.* 68:2333–2341.

Dibble, A. R. G., A. K. Hinderliter, J. J. Sando, and R. L. Biltonen. 1996. Lipid lateral heterogeneity in phosphatidylcholine/phosphatidylserine/diacylglycerol vesicles and its influence on protein kinase C activation. *Biophys. J.* 71:1877–1890.

Fery-Forgues, S., J. Fayet, and A. Lopez. 1993. Drastic changes in the fluorescence properties of NBD probes with the polarity of the medium: involvement of a TICT state? *J. Photochem. Photobiol. A Chem.* 70: 229–243.

Gliss, C., H. Schaumann-Clausen, D. Simson, R. Guenther, S. Odenbach, O. Randl, and T. M. Bayerl. 1998. Direct detection of domains in phospholipid bilayers by grazing incidence diffraction of neutrons and atomic force microscopy. *Biophys. J.* 74:A12.

Hollars, C. W., and R. C. Dunn. 1998. Submicron structure in L-α-dipalmitoylphosphatidylcholine monolayers and bilayers probed with confocal, atomic force, and near-field microscopy. *Biophys. J.* 75: 342–353.

Holopainen, J. M., J. Y. A. Lehtonen, and P. K. J. Kinnunen. 1997. Lipid microdomains in dimyristoylphosphatidylcholine-ceramide liposomes. *Chem. Phys. Lipids.* 88:1–13.

Hønger, T., K. Jørgensen, R. L. Biltonen, and O. G. Mouritsen. 1996. Systematic relationship between phospholipase A_2 activity and dynamic lipid bilayer microheterogeneity. *Biochemistry.* 35:9003–9006.

Hwang, J., L. A. Gheber, L. Margolis, and M. Edidin. 1998. Domains in cell plasma membranes investigated by near-field scanning optical microscopy. *Biophys. J.* 74:2184–2190.

Jørgensen, K., A. Klinger, M. Braiman, and R. L. Biltonen. 1996. Slow nonequilibrium dynamical rearrangement of the lateral structure of a lipid membrane. *J. Phys. Chem.* 100:2766–2769.

Jørgensen, K., M. M. Sperotto, O. G. Mouritsen, J. H. Ipsen, and M. J. Zuckermann. 1993. Phase equilibria and local structure in binary lipid bilayers. *Biochim. Biophys. Acta.* 1152:135–145.

Karlsson, O. P., M. Rytomaa, A. Dahlqvist, P. K. J. Kinnunen, and A. Wieslander. 1996. Correlation between bilayer lipid dynamics and activity of the diglucosyldiacylglycerol synthase from *Acholeplasma laidlawii* membranes. *Biochemistry.* 35:10094–10102.

Knoll, W., K. Ibel, and E. Sackmann. 1981. Small-angle neutron scattering study of lipid phase diagrams by contrast variation method. *Biochemistry.* 20:6379–6383.

Korlach, J., P. Schwille, W. W. Webb, and G. W. Feigenson. 1999. Characterization of lipid bilayer phases by confocal microscopy and fluorescence correlation spectroscopy. *Proc. Natl. Acad. Sci. U.S.A.* 96:8461–8466.

Lehtonen, J. Y. A., J. M. Holopainen, and P. K. J. Kinnunen. 1996. Evidence for the formation of microdomains in liquid crystalline large unilamellar vesicles caused by hydrophobic mismatch of the constituent phospholipids. *Biophys. J.* 70:1753–1760.

Loura, L. M. S., F. Aleksandre, and M. Prieto. 2000. Partition of membrane probes in a gel/fluid two-component lipid system: a fluorescence energy transfer study. *Biochim. Biophys. Acta.* 1467:101–112.

Mabrey, S., and J. M. Sturtevant. 1976. Investigation of phase transitions of lipids and lipid mixtures by high sensitivity differential scanning calorimetry. *Proc. Natl. Acad. Sci. U.S.A.* 73:3862–3866.

Melo, E. C. C., I. M. G. Lourtie, M. B. Sankaram, T. E. Thompson, and W. L. C. Vaz. 1992. Effects of domain connection and disconnection on the yields of in-plane biomolecular reactions in membranes. *Biophys. J.* 63:1506–1512.

Mendelsohn, R., and C. C. Koch. 1980. Deuterated phospholipids as Raman spectroscopy probes of membranes. *Biochim. Biophys. Acta.* 598:260–271.

Mendelsohn, R., G. L. Liang, H. L. Strauss, and R. G. Snyder. 1995. IR spectroscopic determination of gel state miscibility in long-chain phosphatidylcholine mixtures. *Biophys. J.* 69:1987–1998.

Mendelsohn, R., and D. J. Moore. 1998. Vibrational spectroscopic studies of lipid domains in biomembranes and model systems. *Chem. Phys. Lipids.* 96:141–157.

Mesquita, M. M. R. S., E. Melo, T. E. Thompson, and W. L. C. Vaz. 2000. Partitioning of amphiphiles between coexisting ordered and disordered phases in two-phase lipid bilayer membranes. *Biophys. J.* 78: 3019–3025.

Möhwald, H., C. Dietrich, G. Böhm, G. Brezesinski, and M. Thoma. 1995. Domain formation in monolayers. *Mol. Membr. Biol.* 12:29–38.

Mouritsen, O. G., and K. Jørgensen. 1994. Dynamical order and disorder in lipid bilayers. *Chem. Phys. Lipids.* 73:3–25.

Mouritsen, O. G., and K. Jørgensen. 1997. Small-scale lipid-membrane structure: simulation versus experiment. *Curr. Opin. Struct. Biol.* 7:518–527.

Mukherjee, S., T. T. Soe, and F. R. Maxfield. 1999. Endocytic sorting of lipid analogues differing solely in the chemistry of their hydrophobic tails. *J. Cell Biol.* 144:1271–1284.

Nichols, J. W., and R. E. Pagano. 1981. Kinetics of soluble lipid monomer diffusion between vesicles. *Biochemistry.* 20:2783.

Nielsen, L. K., A. Vishnyakov, K. Jørgensen, T. Bjørnholm, and O. G. Mouritsen. 2000. Nano-meter-scale structure of fluid lipid membranes. *J. Phys. Condens. Matter.* 12:A309–A314.

Oliver, A. E., G. A. Baker, R. D. Fugate, F. Tablin, and J. H. Crowe. 2000. Effects of temperature on calcium-sensitive fluorescence probes. *Biophys. J.* 78:2116–2126.

Pedersen, S., K. Jørgensen, T. R. Bækmark, and O. G. Mouritsen. 1996. Indirect evidence for lipid-domain formation in the transition region of phospholipid bilayers by two-probe fluorescence energy transfer. *Biophys. J.* 71:554–560.

Ruggiero, A., and B. Hudson. 1989. Critical density fluctuations in lipid bilayers detected by fluorescence lifetime heterogeneity. *Biophys. J.* 55:1111–1124.

Sankaram, M. B., D. Marsh, and T. E. Thompson. 1992. Determination of fluid and gel domain sizes in two-component, two-phase lipid bilayers: an electron spin resonance spin label study. *Biophys. J.* 63:340–349.

Schram, V., H. N. Lin, and T. E. Thompson. 1996. Topology of gel-phase domains and lipid mixing properties in phase-separated two-component phosphatidylcholine bilayers. *Biophys. J.* 71:1811–1822.

Silvius, J. R., D. del Guidice, and M. Lafleur. 1996. Cholesterol at different bilayer concentrations can promote or antagonize lateral segregation of phospholipids of different acyl chain length. *Biochemistry.* 35: 15198–15208.

Stillwell, W., L. J. Jenski, M. Zerouga, and A. C. Dumaual. 2000. Detection of lipid domains in docosahexanoic acid-rich bilayers by acyl chain-specific FRET probes. *Chem. Phys. Lipids.* 104:113–132.

Stryer, L. 1978. Fluorescence energy transfer as a spectroscopic ruler. *Annu. Rev. Biochem.* 47:819–846.

Sugar, I. P., T. E. Thompson, and R. L. Biltonen. 1999. Monte Carlo simulation of two-component bilayers: DMPC/DSPC mixtures. *Biophys. J.* 76:2099–2110.

Vaz, W. L. C., E. C. C. Melo, and T. E. Thompson. 1990. Fluid phase connectivity in an isomorphous, two-component, two-phase phosphatidylcholine bilayer. *Biophys. J.* 58:273–276.

Verkade, P., and K. Simons. 1997. Lipid microdomains and membrane trafficking in mammalian cells. *Histochem. Cell Biol.* 108:211–220.

Welti, R., and M. Glaser. 1994. Lipid domains in model and biological membranes. *Chem. Phys. Lipids.* 73:121–137.